Springer

Journal of Mechanical Science and Technology 23 (2009) 3095~3104

Journal of Mechanical Science and Technology

www.springerlink.com/content/1738-494x
DOI 10.1007/s12206-009-0813-6

Two-phase flow heat transfer of R-134a in microtubes †

Yun Wook Hwang and Min Soo Kim*

School of Mechanical and Aerospace Engineering, Seoul National University, Seoul, 151-742, Korea

(Manuscript Received September 28, 2007; Revised February 8, 2009; Accepted July 28, 2009)

Abstract

The characteristics of the two-phase flow heat transfer of R-134a in microtubes with inner diameters of 430 μm and 792 μm were experimentally investigated. The effect of the heat flux on the heat transfer coefficient for microtubes was significant before the transition quality. The boiling number expressed the interrelation between the heat flux and the mass about the heat transfer coefficients. The smaller microtube had greater heat transfer coefficients; the average heat transfer coefficient for the tube A (D_i = 430 μm) was 47.0% greater than that for the tube B (D_i = 792 μm) at G = 370 kg/m^2·s and q'' = 20 kW·m^2. A new correlation for the evaporative heat transfer coefficients in microtubes was developed by considering the following factors: the laminar flow heat transfer coefficient of liquid-phase flow, the enhancement factor of the convective heat transfer, and the nucleate boiling correction factor. The correlation developed in present study predicted the experimental heat transfer coefficients within an absolute average deviation of 8.4%.

Keywords: Microtube; Two-phase flow; Evaporation; Heat transfer coefficient; Correlation

1. Introduction

Many electronic devices have become smaller and lighter so heat dissipation has been one of the main considerations in designing these devices because heat density, which is the heat generation per unit volume, has continued to increase even if the total heat generation itself has decreased thanks to the advances of the electronic circuit technology. Thus, effectively removing and controlling the heat generation has been a challenging task and heat transfer engineering is playing a key role in this field.

It is obvious that the restriction of the space of smaller electronic devices requires cooling systems equipped with microchannels in order to operate in normal condition. Cooling systems can use single-phase fluid or two-phase fluid as a coolant. For single-phase flow, the flow rate should be increased or the hydraulic diameter should be decreased in order to remove increased heat generation. Both methods are susceptible to great pressure drop. However, the two-phase flow under evaporation can give more uniform surface temperature than the single-phase flow and remove much more heat because the heat transfer coefficient of the two-phase flow is much greater than that of the single-phase flow. The flow boiling gives greater heat transfer coefficients, and thus can make possible smaller heat exchangers.

Many studies on the heat transfer in micro geometries have been done until now (Tuckermann [1], Wu and Little [2], Choi *et al.* [3], Peng and Wang [4], Mudawar and Bowers [5], Peng *et al.* [6], Wang and Peng [7], Peng and Petterson [8], Arlilic *et al.* [9], Peng *et al.* [10], Ravigururajan [11], Adams *et al.* [12], Zaho *et al.* [13]). The studies of Peng and Wang [4], Mudawar and Bowers [5], Peng *et al.* [10], Ravigururajan [11], and Zaho *et al.* [13] were about two-phase flow heat transfer and the others were about single-phase flow heat transfer. Peng and Wang [4] investigated the characteristics of the subcooled boiling of liquid flowing through microchannels with a cross-section of 0.6 × 0.7 mm, machined on the

† This paper was recommended for publication in revised form by Associate Editor Jae Young Lee

*Corresponding author. Tel.: +82 2 880 8362, Fax.: +82 2 883 0179
E-mail address: minskim@snu.ac.kr

stainless steel plate of 2 mm thickness and found that no apparent partial nucleate boiling existed for subcooled flow boiling, and fully-developed boiling was induced much earlier in microchannels. Mudawar and Bowers [5] performed an experimental study on the CHF in mini-channel (D_i = 2.54 mm) and microchannel (D_i = 510 μm) and showed that the CHF values could reach 200 W/cm^2 with the advantage of both low flow rates and low pressure drops. Peng *et al.* [10] analyzed the thermodynamic aspects of phase transition in microchannels and theoretically derived the nondimensional parameter that determined the phase transition in microchannels. Raviguruajan [11] tested the parallel pattern microchannel and the diamond pattern microchannel. He showed that the heat transfer coefficient decreased from 12 kW/m^2·K to 9 kW/m^2·K at 80^{o}C when the wall superheat is increased from 10 to 80^{o}C. Zhao *et al.* [13] conducted experiments on the flow boiling of CO_2 in microchannels at mass fluxes of 250 to 700 kg/ m^2·s and heat fluxes of 8 to 25 kW/m^2. They showed that the heat transfer coefficient of CO_2 in microchannels is almost independent of heat flux and mass flux, and CO_2 offers outstanding heat transfer characteristics compared to traditional refrigerants such as R-134a.

It is generally known that the effect of the surface tension becomes greater as the channel gets smaller. Greater surface tension in the microchannels increases capillary force, which can result in the change of the void fraction, liquid film distribution, etc. Capillary bubble flows can arise for extremely small tubes and the vapor bubble completely may fill the cross section, leaving the wall at that location dry (Carey [14]). Although the transport phenomena in the microchannels may be different from that in the conventional tubes, little has been known about the pressure drop and the heat transfer under evaporation in the microchannels.

The test sections used in the existing studies on the two-phase flow heat transfer were mostly the multi-microchannels. Even if the micro heat exchangers can be manufactured with multichannels, the performance of a single test tube needs to be investigated in order to verify the characteristics of the heat transfer itself because the test results in the mutli-microchannels may include the effects of the diverse geometries on the heat transfer. In addition, the test fluids adopted in the existing studies were nitrogen, helium, de-ionized water, methanol, R-113, etc., which are the gases or the liquids which are all low in pressure. Therefore, in present study, the two-phase flow heat transfer in single microtubes is experimentally investigated and theoretically analyzed using R-134a as a test fluid. Also, based on the measured experimental results, the correlation to predict the two-phase flow heat transfer coefficients in microtubes is proposed in the form of the enhancement model.

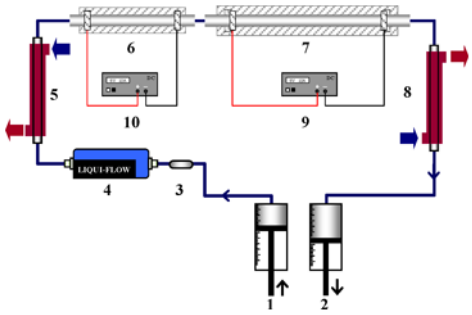

Fig. 1. Experimental test rig for the two-phase flow heat transfer test (1: syringe pump 1, 2: syringe pump 2, 3: filter, 4: thermal mass flow meter, 5: subcooler, 6: preheater, 7: test section, 8: condenser, 9: DC power supply for preheater, 10: DC power supply for test section).

2. Experiments

2.1 Experimental test rig

Fig. 1 shows the schematic diagram of the experimental test rig built for the heat transfer test. It has two syringe pumps, filter, mass flow meter, subcooler, preheater, test section, and condenser. The syringe pump 1 discharges the test fluid at a constant flow rate. The thermal mass flow meter measures the mass flow rate of the test fluid into the test section. The subcooler and the preheater control the inlet quality of the test fluid flowing into the test section. The DC power supply (HP 6733A) is used to provide the accurate amount of the electric power to the test fluid in the preheater. The test fluid in saturation state flows into the test section and experiences evaporation by the electric heat provided by the DC power supply (Agilent 6651A). The condenser makes the test fluid exiting the test section back to the subcooled state, and then it flows into the syringe pump 2, which keeps the test system at constant pressure during the heat transfer test by changing the cylinder volume

2.2 Test sections

Two kinds of microtubes are used to investigate the heat transfer characteristics in the microtubes and their diameters and lengths are listed in Table 1.

Table 1. Specifications of the test sections for the two-phase flow heat transfer test.

Test tube	D_i (μm)	L (mm)
A	430	60
B	792	90

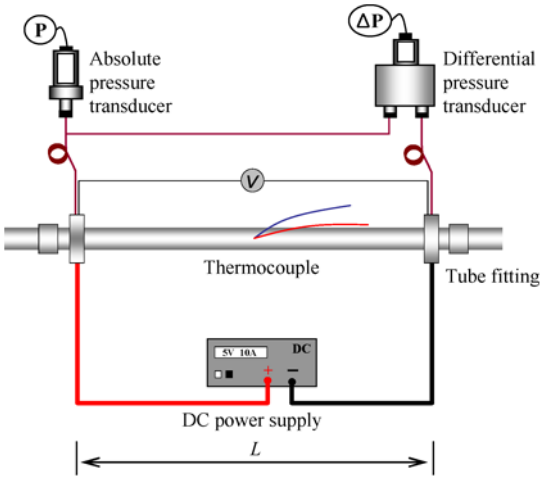

Fig. 2. Detailed view of the test section.

The direct heating method is employed to provide heat to the test fluid flowing in the test section. It has an advantage to accurately adjust the voltage or the current applied to the test section. Fig. 2 shows the electric power supply system to the test section.

Thin thermocouples are used for temperature measurement at the mid-point of the test section. A thin layer of the Teflon tape was wound around the test section in order to electrically insulate the thermocouple from the electric current in the test section. Then, the thermocouples were placed onto the Teflon layer. Two layers of ceramic fiber insulator and rubber foaming insulator thermally insulate the test section to prevent the heat transfer between the test fluid in the test section and the ambient atmosphere.

The local pressure should be measured in order to calculate the heat transfer coefficient because the saturation temperature can be determined by the saturation pressure of the test fluid during the two-phase flow heat transfer test. As shown in Fig. 2, the absolute pressure transducer installed at the inlet of the test section measures the inlet pressure of the test fluid and the differential pressure transducer measures the pressure drop over the test section. The local pressure is calculated with the inlet pressure and the pressure drop (see Eq. (1)).

Table 2. Test conditions for the two-phase flow heat transfer test.

Test tube	G (kg/m^2·s)	q'' (kW/m^2)
A	110, 240, 370	5 – 40
B	240, 370, 640	15 – 40

$$p_z = p_{t,in} + \frac{\Delta p}{L} \times z \tag{1}$$

where p_z is local pressure, $p_{t,in}$ is inlet pressure, Δp is pressure drop, and L is the length of the test section.

2.3 Test condition

Table 2 shows the test conditions for the two-phase flow heat transfer test. Two kinds of microtubes are used as a test section for the two-phase flow heat transfer test at various mass flux(G), heat flux(q''), and the quality conditions. The heat flux is varied by the DC power supply and the mass flux is varied by the syringe pump 1 shown in Fig. 1.

3. Experimental results and discussion

3.1 Data reduction and verification

The evaporative heat transfer coefficient is defined as the heat flux divided by the wall superheat.

$$h = \frac{q''}{T_i - T_{sat}} \tag{2}$$

where h is two-phase flow heat transfer coefficient, q'' is heat flux, T_i is inner wall temperature, and T_{sat} is the saturation temperature.

The heat flux is the heat divided by the inner surface area of the test section. The supplied heat is assumed to be the same as the electric energy and is expressed as the product of the DC voltage and the current. The inner wall temperature is calculated with the measured outer wall temperature by using the one dimensional heat conduction equation with heat generation inside the tube wall (see Eq. (3)).

$$T_i = T_o + \frac{\dot{q} D_o^2}{16\lambda}\left(1 - \frac{D_i^2}{D_o^2}\right) + \frac{\dot{q} D_o^2}{8\lambda}\ln\left(\frac{D_i}{D_o}\right) \tag{3}$$

where T_o is outer wall temperature, $\dot{q}$ is heat generation per unit volume, D_i is inner diameter, D_o is outer

diameter, and λ is the thermal conductivity of the test section.

In the evaporative heat transfer test, the saturation pressure determines the saturation temperature. The local saturation pressure is calculated with the pressure at the inlet of the test section and the pressure drop along the test section.

The quality is calculated from the energy balance between the energy input by the electricity and the energy absorbed by the test fluid, which is expressed in Eq. (4). It is mass quality at the mid-point of the test section like wall temperature measurement because the test section was uniformly heated through direct heating method.

$$x = \frac{\left(V_p \cdot I_p + V_t \cdot I_t / 2\right)/\dot{m} + i_{f,p,in} - i_{f,t,in}}{i_{fg,t,in}} \tag{4}$$

where V_p is voltage at the preheater, V_t is voltage at the test section, I_p is current at the preheater, I_t is current at the test section, $\dot{m}$ is mass flow rate, $i_{f,p,in}$ is saturation liquid enthalpy at the preherater inlet, $i_{f,t,in}$ is saturation liquid enthalpy at the test section inlet, and $i_{fg,t,in}$ is the enthalpy difference between saturation liquid and saturation vapor at the test section inlet.

An energy balance was done in order to estimate the accuracy of the heat transfer measurement. The power input(E_{meas}) denoted by Eq. (5) is the product of the voltage between both ends of the test section and the electric current flowing through it. The energy(E_{cal}) absorbed by the test fluid is calculated by the following Eq. (6).

$$E_{meas} = V_t \cdot I_t \tag{5}$$

$$E_{cal} = \dot{m} \cdot (i_{t,out} - i_{t,in}) \tag{6}$$

where $i_{t,in}$ and $i_{t,out}$ are the enthalpies of test fluid entering and exiting the test section, respectively. The enthalpy is calculated by REFPROP (Lemmon *et al.* [15]) with the measured pressure and the temperature. The absolute average deviation between the power input and the energy gain was 4.9%.

An uncertainty analysis was done for the measurement of the evaporative heat transfer coefficients according to the procedures described by Coleman and Steele [16], and the uncertainty of the evaporative heat transfer coefficient ranged from 4.9 to 15.5% for the test tube A (D_i = 430 μm) and from 2.7 to 17.9% for the test tube B (D_i = 792 μm).

3.2 Heat transfer characteristics

Fig. 3 shows the heat transfer coefficient for the test tube A (D_i = 430 μm) versus quality at G = 240 kg/m^2·s. The variation of the heat flux has a significant effect on the heat transfer coefficient before the transition quality, which seems to be about 0.7. The difference among the heat transfer coefficients is very small beyond the transition quality. In general, the nucleate boiling is enhanced when the heat flux is great and the mass flux is small because the nucleate boiling is not so well suppressed. The heat transfer coefficient decreases with increasing quality and the heat transfer beyond the transition quality is dominated by the convective boiling. The nucleate boiling is not so well-enhanced at q'' = 15 kW/m^2 and q'' = 20 kW/m^2 as that at q'' = 30 kW/m^2.

Fig. 4 shows the heat transfer coefficient for the test tube B (D_i = 792 μm) versus quality at G = 110 kg/m^2·s. The trend of the heat transfer coefficient versus the heat flux is similar to that for the test tube A (D_i = 430 μm). The effect of the heat flux is

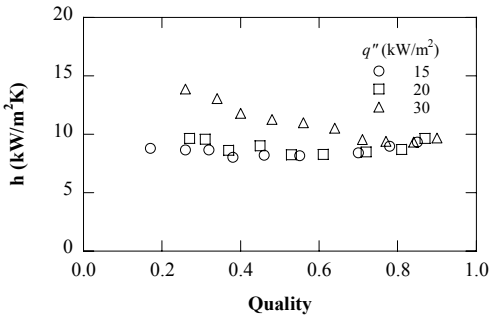

Fig. 3. Evaporative heat transfer coefficients versus quality with respect to the variation of the heat flux for the test tube A (D_i = 430 μm) at G = 240 kg/m^2·s.

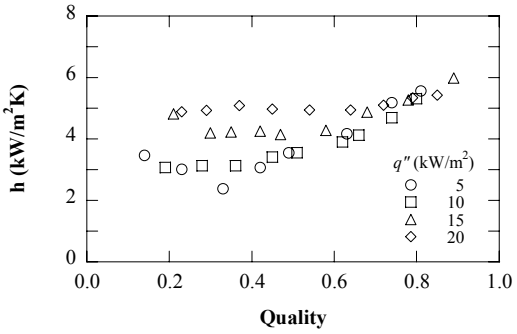

Fig. 4. Evaporative heat transfer coefficients versus quality with respect to the variation of the heat flux for the test tube B (D_i = 792 μm) at G =110 kg/m^2·s.

significant at the low quality region. Lee and Lee [17] studied the two-phase flow heat transfer for the rectangular channels using R-113. They found that the heat flux has a minor effect on the boiling heat transfer and the two-phase forced convection is considered to be the predominant mechanism in the heat transfer. It is true that the heat flux has a minor effect on the heat transfer at the high quality region. However, they did not show the variation of the heat transfer coefficient at the low quality region with respect to the heat flux.

Fig. 5 shows the effect of the mass flux on the heat transfer coefficient for the test tube A (D_i = 430 μm) versus the quality at q'' =30 kW/m^2. The mass flux has little effect on the variation of the heat transfer coefficient at the low quality region. The difference between the heat transfer coefficients becomes wider with increasing quality because the mean velocity of the test fluid increases. As the phase-change continues, the mass fraction of the vapor phase increases, so the average density of the two-phase flow decreases.

Fig. 6 shows the heat transfer coefficients versus the quality for the test tube A (D_i = 430 μm) when the boiling numbers are similar to each other. When the boiling numbers are 4.425×10^{-4} and 4.344×10^{-4}, respectively, the trends of the heat transfer coefficient versus the quality are quite similar to each other even if the magnitude of the heat transfer coefficient is quite different. As seen in Fig. 7, the trends of the heat transfer coefficient versus the quality for the test tube B (D_i = 792 μm) are quite similar to each other. Therefore, the boiling number is considered to be a very important parameter to predict the trend of the heat transfer coefficients versus the quality even if it does not determine the magnitude of the heat transfer coefficients.

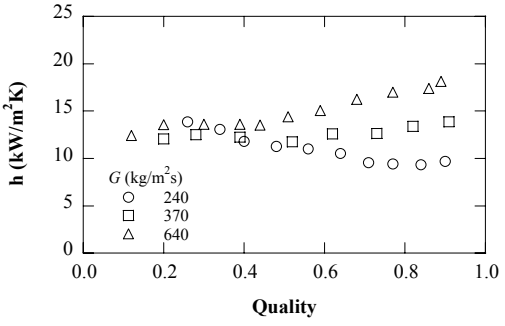

Fig. 5. Evaporative heat transfer coefficients versus quality at q'' = 30 kW/m^2 with respect to the variation of the mass flux for the test tube A (D_i = 430 μm).

3.3 Effect of tube diameter

The heat transfer coefficients for the test tube with an inner diameter of 7.75 mm by Choi *et al.* [18] were compared with the experimental data results for the test tube A (D_i = 430 μm) and the test tube B (D_i =

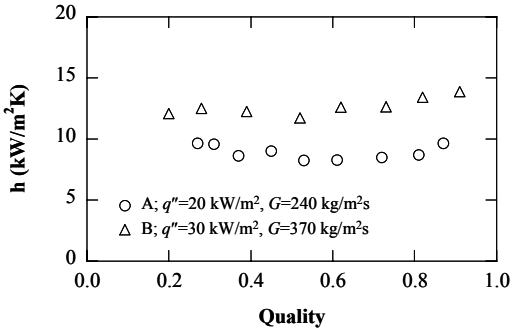

Fig. 6. Evaporative heat transfer coefficients versus quality for the test tube A (D_i = 430 μm) when the boiling numbers are similar to each other (A: Bo=4.425×10^{-4}; B: Bo=4.344×10^{-4}).

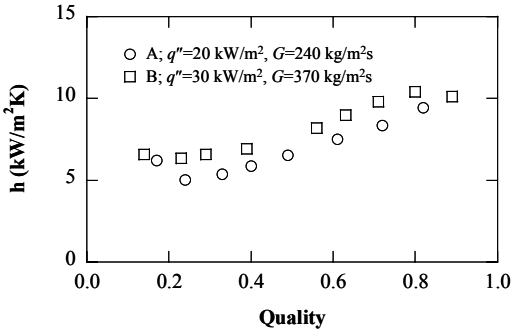

Fig. 7. Evaporative heat transfer coefficients versus quality for the test tube B (D_i = 792 μm) when the boiling numbers are similar to each other (A: Bo=4.577×10^{-4}; B: Bo=4.488×10^{-4}).

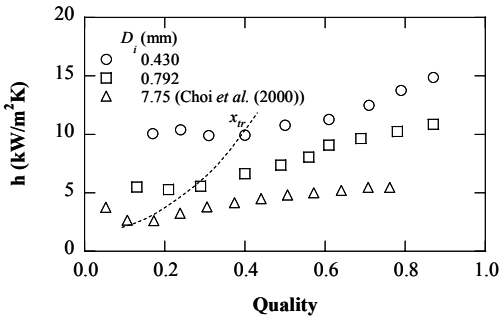

Fig. 8. Heat transfer coefficients with respect to the variation of the tube diameter at q'' ≈ 20 kW/m^2 and G = 427 kg/m^2·s for Choi *et al.* [18] and 370 kg/m^2·s for the test tube A (D_i = 430 μm) and the test tube B (D_i = 792 μm).

Table 3. The difference between the heat transfer coefficients for the test tube A (D_i = 430 μm) and the test tube B (D_i = 792 μm).

G (kg/m^2·s)	q'' (kW/m^2)	$\frac{h_{m,A}-h_{m,B}}{h_{m,B}}\times 100(\%)$
240	20	31.5
	30	52.1
370	20	47.0
	30	53.8

where $h_{m,A}$, and $h_{m,B}$ are average heat transfer coefficients for the test section A and B, respectively.

792 μm) at almost the same test condition. Fig. 8 clearly shows that the smaller the tube, the greater the heat transfer coefficients even though the heat flux is almost the same but the mass flux is a little different among them. The average heat transfer coefficients for the test tube A (D_i = 430 μm) and the test tube B (D_i = 792 μm) are about 171.8% and 84.9% greater than that for the test tube by Choi *et al.* [18].

Table 3 lists the difference between the average heat transfer coefficients for the test tube A (D_i = 430 μm) and the test tube B (D_i = 792 μm). It changes from 32.5% to 52.1% when the heat flux is varied from 20 kW/m^2 to 30 kW/m^2 at G = 240 kg/m^2·s. Also, the difference between the average heat transfer coefficients changes from 47.0% to 53.8% at G = 370 kg/m^2·s.

The fluid flow in the smaller tubes has a thinner thermal boundary layer because the thermal boundary layer is the distance between the tube surface and the center of the tube. Therefore, the fluid flow in the smaller tubes can have greater heat transfer coefficients as obtained in this study. The nucleation in the smaller tubes can be enhanced because the bubble occupies larger volume or cross sectional area of the flow area, so the bubble actively agitates the movement of the superheated liquid during the growth and the detachment of the bubble. The heat transfer is enhanced from the viewpoint of the convection and the nucleation. Also, Fig. 8 shows that the transition quality(x_{tr}) becomes high as the tube diameter decreases, which means that the nucleation effect on the two-phase heat transfer extends to the high quality region due to smaller Reynolds number and convection effect.

4. Heat transfer correlation

The experimental heat transfer coefficients were compared with the six existing correlations. Table 4 shows the comparisons between the experimental heat transfer coefficients for the test tube A (D_i = 430 μm) and the predicted heat transfer coefficients. The Gungor and Winterton [19] correlation predicts the heat transfer coefficients better than other correlations even if all correlations underpredict the two-phase flow heat transfer coefficients in the microtubes. Although the Lee and Lee [17] correlation was developed with the microchannels having a low aspect ratio, its absolute average deviation is up to 162.2%. It is because they ignored the effect of the heat flux on the heat transfer, which was found not negligible in this study, and the test conditions are different from each other. Their tests were conducted at the test conditions of the low mass flux and the low heat flux. The mass flux and the heat flux in the micro geometries are considered to be comparable to or somewhat greater than those in the conventional-sized flow channels. On the contrary, Tran *et al.* [21] ignored the effect of the mass flux on the heat transfer, which was found to be significant in the microtubes. Its absolute average deviation is up to 76.9%. The Kandlikar [22] correlation using the all-liquid flow heat transfer coefficient, h_{LO}, by Dittus-Boelter [24] underpredicted the experimental heat transfer coefficients by 33.6% because it was developed with conventional-sized tubes and did not consider laminar flow regime in microchannels. The Kandlikar and Balasubramanian [23] correlation, which extended the Kandlikar [22] correlation to laminar flow in microchannels, also underpredicted the experimental heat transfer coefficients by 62.9%. It failed to predict the experimental heat

Table 4. The deviations between the experimental heat transfer coefficients for the test tube A (D_i = 430 μm) and the test tube B (D_i = 792 μm) and the predicted heat transfer coefficients with the existing correlations.

Correlation	Test tube A		Test tube B	
	σ_a	σ_{aa}	σ_a	σ_{aa}
Gungor and Winterton [19]	-28.2	28.2	-17.4	20.9
Jung *et al*. [20]	-45.1	45.1	-33.2	33.7
Tran *et al*. [21]	-76.9	76.9	-56.7	56.7
Lee and Lee [17]	162.2	162.2	174.1	174.1
Kandlikar [22]	-33.6	33.6	-26.0	26.0
Kandlikar and Balasubramanian [23]	-62.9	62.9	-54.0	54.0

where σ_a and σ_{aa} are average deviation and absolute average deviation, respectively.

transfer coefficients because the Kandlikar and Balasubramanian [23] correlation was not developed with experimental data for micro geometries and just substituted all-liquid flow heat transfer coefficient, h_{LO}, with single-phase laminar flow heat transfer coefficients. Figs. 9 and 10 show the comparison of the Kandlikar [22] correlation using single-phase laminar heat transfer coefficients, which are calculated from constant Nusselt number of laminar flow, with experimental heat transfer data. In Fig. 9, the Kandlikar [22] correlation with single-phase flow heat transfer coefficients expected that h/ h_{LO} changed little with increasing quality and has little dependence on variation of heat flux. However, experimental h/ h_{LO} decreases as heat flux increases and is greatly enhanced at high heat flux condition. Fig. 10 also shows that the Kandlikar [22] correlation failed to expect the increasing trend of h/ h_{LO} versus quality at high quality region.

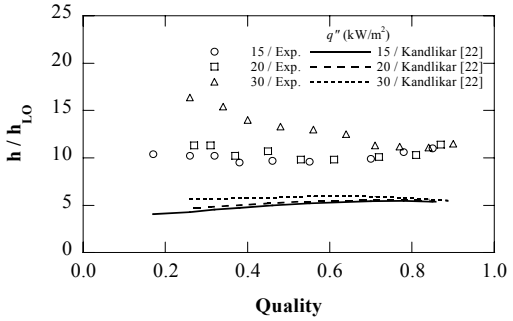

Fig. 9. Comparison of experimental heat transfer coefficients for the test tube A (D_i = 430 μm) at G = 240 kg/m^2·s with Kandlikar [22] correlation using single-phase laminar heat transfer coefficients.

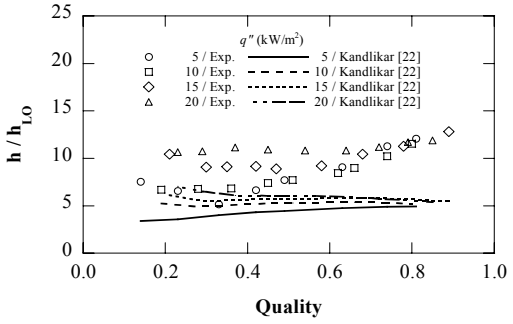

Fig. 10. Comparison of experimental heat transfer coefficients for the test tube B (D_i = 792 μm) at G = 110 kg/m^2·s with Kandlikar [22] correlation using single-phase laminar heat transfer coefficients.

Table 4 also shows the comparisons between the experimental heat transfer coefficients for the test tube B (D_i = 792 μm) and the predicted heat transfer coefficients. It is clear that the existing correlations predict the heat transfer coefficients for the test tube B (D_i = 792 μm) better than those for the test tube A (D_i = 430 μm). The change of the tube diameter is reflected only in the convection heat transfer term of the existing correlations. As described in foregoing section, the change of the tube diameter can have an effect on the nucleate boiling heat transfer term. It is generally known that the surface tension effect becomes big as the flow channel dimension decreases. Therefore, the relative effect of surface tension on the change of the tube diameter, which can be expressed by confinement number, N_{conf}, should be included in the newly-developed correlation.

The experimental results showed that the heat transfer at the nucleation-dominating region is strongly affected by the heat flux, and the mass flux has a negligible effect on the heat transfer. On the other hand, the heat transfer at the convection-dominating region is strongly affected by the mass flux and the flux has a negligible effect on the heat transfer. Therefore, the correlation for the two-phase flow heat transfer in micro tubes is modeled as shown in Eq. (7).

$$h = \mathrm{Max}\left\{h_{CO}, h_{NB}\right\} = \mathrm{Max}\left\{F \cdot h_l, S \cdot h_{pool}\right\} \tag{7}$$

h_{CO} is the convective heat transfer coefficient and can be expressed as the product of the heat transfer coefficient of the liquid-phase (h_l) and the enhancement factor(F). The existing correlations were developed mostly for the larger-sized tubes. In addition, the flow regime of the liquid flow was assumed to be turbulent, so they used Dittus-Boelter [24] correlation or Gnielinski [25] correlation to obtain the heat transfer coefficient of the liquid-phase (h_l). The flow regimes in micro geometries are laminar due to the small flow passage. From the heat transfer theory for fully-developed laminar flow, the Nusselt number is 4.36 for constant heat flux boundary condition and 3.66 for the constant wall temperature heat flux condition. However, the heat exchangers equipped with the microchannels mostly have multichannels and each flow channel can be short because a long channel is subject to high pressure drop. It is possible that the thermal boundary is developing, not fully-developed in the micro heat exchangers. Therefore,

the heat transfer coefficient of the liquid-phase needs to be calculated with the equation for the laminar-flow. The theoretical relation by Kays and Crawford [26] was used to obtain the heat transfer coefficient of the liquid-phase. The necessary eigenvalues and constants are given in Table 5.

$$\mathrm{Nu}_z = \left[\frac{1}{\mathrm{Nu}_\infty} - \frac{1}{2} \sum_{m=1}^{\infty} \frac{\exp\left(-\gamma_m^2 z^+\right)}{A_m \gamma_m^4} \right]^{-1} \tag{8}$$

where Nu_z is local Nusselt number, Nu_∞ is Nusselt number of fully-developed laminar flow under constant heat flux, and γ_m and A_m are coefficients.

Chen [27] developed a two-phase flow heat transfer correlation based on the superposition model. He later showed that the multiplier, F, can be expressed as the functional form of the two-phase frictional multipliers based on the pressure gradient for liquid-phase flow. Therefore, the enhancement factor, which was called as the multiplier by Chen [27], is correlated with the two-phase frictional multipliers based on the pressure gradient for liquid-phase flow. The two-phase frictional multipliers were calculated by using the experimental correlation, which was given by Hwang and Kim [28].

$$F = C_0 \times \left(\phi_f^2\right)^{C_1} \tag{9}$$

h_{NB} is the nucleate boiling heat transfer coefficient and can be expressed as the product of the pool boiling heat transfer coefficient (h_{pool}) and the nucleate boiling correction factor (S). The Cooper [29] correlation for pool boiling heat transfer is used to obtain the nucleate boiling heat transfer coefficient. The nucleate boiling correction factor, S, accounts for the difference between the pool boiling and the flow boiling. It can include the effects of the heat flux, mass flux, thermophysical properties, tube diameter, quality, and so on. Therefore, the nucleate boiling correction factor can be expressed in the following form shown in Eq. (10).

$$S = C_2 \times \left(Bo\right)^{C_3} \times \left(N_{conf}\right)^{C_4} \times X^{C_5} \tag{10}$$

The boiling number, Bo, includes the effects of the heat flux and the mass flux. The confinement number, N_{conf}, can reflect the relative effect of surface tension to the change of the tube diameter, and the Martinelli parameter reflects the change of the quality.

Table 5. The coefficients of the proposed correlation for the two-phase flow heat transfer coefficients in this study.

Test tube	G (kg/m^2·s)	q'' (kW/m^2)
A	110, 240, 370	5 − 40
B	240, 370, 640	15 − 40

G: 110 ~ 640 kg/m^2·s, q'': 5 ~ 40 kW/m^2

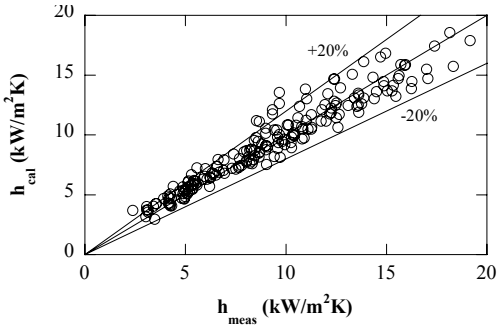

Fig. 11. Comparison of the calculated two-phase flow heat transfer coefficients with the experimental two-phase flow heat transfer coefficients.

A regression analysis for 191 experimental data calculates C_0, C_1, C_2, C_3, C_4, and C_5, which are listed in Table 6. The experimental heat transfer coefficients are compared with the newly-developed heat transfer correlation in Fig. 11. The average deviation, absolute average deviation, and the RMS deviation of the measured heat transfer coefficients from the heat transfer coefficients calculated with the new correlation in this study are -2.6%, 8.4%, and 10.7%, respectively.

5. Conclusions

The characteristics of the two-phase flow heat transfer in microtubes have been experimentally investigated and theoretically analyzed. The effect of the heat flux on the heat transfer coefficient for the test tubes was significant before the transition quality. The difference between the heat transfer coefficients was very small beyond the transition quality and the heat transfer was dominated by convection. The boiling number expressed the interrelation between the heat flux and the mass flux about the heat transfer coefficients. When the boiling numbers were similar to each other, the trends of the heat transfer coefficient versus the quality were quite similar to each other. The smaller microtube had greater heat transfer coefficients; the average heat transfer coefficient for

the tube A (D_i = 430 μm) was 47.0% greater than that for the tube B (D_i = 792 μm) at G = 370 kg/m^2·s and q'' = 20 kW/m^2. A new correlation for the evaporative heat transfer coefficients in micro tubes was developed by considering the following factors: the laminar flow heat transfer coefficient of liquid-phase flow, the enhancement factor of the convective heat transfer, and the nucleate boiling correction factor. The correlation developed in this study predicted the experimental heat transfer coefficients for microtubes within an absolute average deviation of 8.4%.

Acknowledgements

This work was jointly supported by the Micro Thermal System Research Center at Seoul National University and the Ministry of Science & Technology (National Research Lab. Program).

References

[1] D. B. Tuckerman, *Heat transfer microstructures for integrated circuits*, PhD thesis, Stanford University, Stanford, CA, 1984.

[2] P. Wu and W. A. Little, Measurement of the heat transfer characteristics of gas flow in fine channel heat exchangers used of microminiature refrigerators, *Cryogenics* 24 (1984) 415-420.

[3] S. B. Choi, R. F. Barron and R. O. Warrington, Fluid flow and heat transfer in microtubes, *Micromechanical Sensors, Actuators, and Systems, ASME DSC*, 1991, pp. 123-134.

[4] X. F. Peng and B. X. Wang, Forced convection and flow boiling heat transfer for liquid flowing through microchannels, *Int. J. Heat Mass Transfer* 36 (1993) 3421-3427.

[5] I. Mudawar and M. B. Bowers, High flux boiling in low flow rate, low pressure drop mini-channel and micro-channel heat sinks, *Int. J. Heat Mass Transfer* 37 (1994) 321-332.

[6] X. F. Peng, G. P. Peterson and B. X. Wang, Heat transfer characteristics of water flowing through microchannels, *Experimental Heat Transfer* 7 (1994) 265-283.

[7] B. X. Wang and X. F. Peng, Experimental investigation on liquid forced convection heat transfer through microchannels, *Int. J. Heat Mass Transfer* 37 (1994) 73-82.

[8] X. F. Peng and G. P. Peterson, The effect of thermofluid and geometrical parameters on convection of liquids through rectangular microchannels, *Int. J. Heat Mass Transfer* 38 (1995) 755-758.

[9] E. B. Arkilic, M. A. Schmidt and K. S. Breuer, Gaseous slip flow in long microchannels, *Journal of Microelectromechanical Systems* 6 (1997) 167-178.

[10] X. F. Peng, H. Y. Hu and B. X. Wang, Boiling nucleation during liquid flow in microchannels, *Int. J. Heat Mass Transfer* 41 (1998) 101-106.

[11] T. S. Ravigururajan, Impact of channel geometry on two-phase flow heat transfer characteristics of refrigerants in microchannel heat exchangers, *J. Heat Transfer* 120 (1998) 485-491.

[12] T. M. Adams, S. I. Abdel-khalik, S. M. Jeter and Z. H. Qureshi, An experimental investigation of single-phase forced convection in microchannels, *Int. J. Heat Mass Transfer* 41 (1998) 851-857.

[13] Y. Zaho, M. Molki, M. M. Ohadi and S. V. Dessiatoun, 2000, Flow boiling of CO2 in microchannels, *ASHRAE Trans.* 106 (2000) DA-00-2-1.

[14] V. P. Carey, 1992, *Liquid-vapor phase-change phenomena: An introduction to the thermophysics of vaporization and condensation processes in heat transfer equipment*, Hemisphere Publishing Corporation, New York, 1992.

[15] E. W. Lemmon, M. O. McLinden and M. L. Huber, *NIST Standard Reference Database 23, NIST reference fluid thermodynamic and transport properties-REFPROP*, Version 7.0, National Institute of Standards and Technology, Boulder, CO, 2002.

[16] H. W. Coleman and W. G. Steele, *Experimentation and uncertainty analysis for engineers*, John Wiley & Sons, New York, 1989.

[17] H. J. Lee and S. Y. Lee, Heat transfer correlation for boiling flows in small rectangular horizontal channels with low aspect ratios, *Int. J. Multiphase Flow* 27 (2001) 2043-2062.

[18] T. Y. Choi, Y. J. Kim, M. S. Kim and S. T. Ro, 2000, Evaporation heat transfer of R-32, R-134a, R-32/134a, and R-32/125/134a inside a horizontal smooth tube , *Int. J. Heat Mass Transfer* 43 (2000) 3651-3660.

[19] K. E. Gungor and R. H. S. Winterton, Simplified general correlation for saturated flow boiling and comparisons of correlations with data, *Chem. Eng. Res. Des.* 65 (1987) 148-156.

[20] D. S. Jung, M. McLinden, R. Radermacher and D. Didion, Horizontal flow boiling heat transfer experiments with a mixture of R22/114, *Int. J. Heat Mass Transfer* 32 (1989) 131-145.

[21] T. N. Tran, M. W. Wambsganss and D. M. France,

Small circular- and rectangular-channel boiling with two refrigerants, *Int. J. Multiphase Flow* 22 (1996) 485-498.

[22] S. G. Kandlikar, A general correlation for saturated two-phase flow boiling heat transfer inside horizontal and vertical tubes, *J. of Heat Transfer* 112 (1990) 219-228.

[23] S. G. Kandlikar and P. Balasubramanian, An extension of the flow boiling correlation to transition, laminar, and deep laminar flows in minichannels and microchannels, *Heat Transfer Engineering* 25 (2004) 86-93.

[24] F. W. Dittus and L. M. K. Boelter, Public engineering, vol. 2, University of California, Berkeley, 1930, p. 443.

[25] V. Gnielinski, New equations for heat and mass transfer in turbulent pipe and channel flow, *Int. Chem. Eng*. 16 (1976) 359-368.

[26] W. M. Kays and M. E. Crawford, *Convective heat and mass transfer*, McGraw-Hill, New York, 1993.

[27] J. C. Chen, Correlation for boiling heat transfer to saturated fluids in convective flow*, I&EC Process Design and Development* 5 (1996) 322-329.

[28] Y. W. Hwang and M. S. Kim, The pressure drop in microtubes and the correlation development, *Int. J. Heat Mass Transfer* 49 (2006) 1804-1812.

[29] M. G. Cooper, Heat flow rates in saturated nucleate pool boiling – a wide-ranging examination using reduced properties, *Advances in Heat Transfer* 16 (1984) 157-239.

Min Soo Kim received his B.S., M.S., and Ph.D. degrees at Seoul National University, Korea in 1985, 1987, and 1991, respectively. After the Ph.D. degree, Prof. Kim worked at the National Institute of Standards and Technology (NIST) in U.S.A. for about three years. He is currently a professor at the School of Mechanical and Aerospace Engineering of Seoul National University, Korea.

Yun Wook Hwang received his B.S., M.S., and Ph.D. from Mechanical Engineering in Seoul National University, Korea in 1997, 1999, and 2004, respectively. Dr. Hwang then worked for the Korea Institute of Machinery and Materials for about three years. He is currently a deputy director at Small and Medium Business Administration of the Korean Government.